Inorganic Chemistry

Article

pubs.acs.org/IC

New Example of Hemiporphycene Formation from the Corrole Ring Expansion

Yuanyuan Fang,[†] Federica Mandoj,[‡] Sara Nardis,[‡] Giuseppe Pomarico,[‡] Manuela Stefanelli,[‡] Daniel O. Cicero,[‡] Sara Lentini,[‡] Andrea Vecchi,[‡] Yan Cui,[†] Lihan Zeng,[†] Karl M. Kadish,*[,†] and Roberto Paolesse*[,‡]

[†]Department of Chemistry, University of Houston, Houston, Texas 77204-5003, United States

[‡]Department of Chemical Science and Technologies, Università di Roma Tor Vergata, 00133 Roma, Italy

Supporting Information

ABSTRACT: The reaction of 5,10,15-tris(4-*tert*-butylphenyl)-corrole with 2,3-bis(bromomethyl)-5,6-dicyanopyrazine provides a new example of corrole ring expansion to a hemiporphycene derivative. The ring expansion is regioselective, with insertion of the pyrazine derivative at the 5-position of the corrole ring, affording the corresponding 5-hemiporphycene. Different macrocyclic products accompany formation of the 5-hemiporphycene, depending on the reaction experimental conditions. Br-substitued 5-hemiporphycenes and the 2-Br substituted corrole were obtained in 1,2,4-trichlorobenzene, while in refluxing toluene traces of an inner core substituted corrole were observed together with a significant amount of the unreacted corrole. These results provide an important indication of the reaction pathway. The coordination behavior of the 5-hemiporphycene, together with detailed electrochemical characterization of the free-base and some metal complexes, provides evidence for the reactivity of the peripheral pyrazino group.

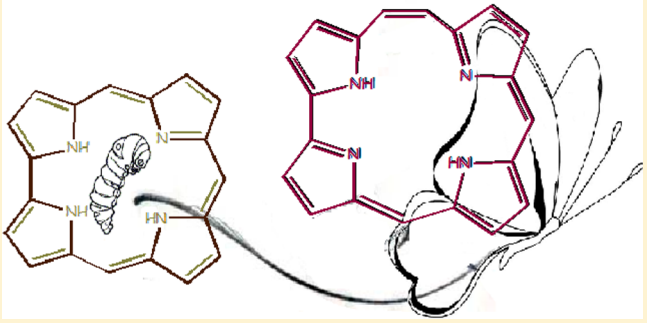

INTRODUCTION

In the past few years, corroles have emerged as important compounds in the porphyrinoids arena, since their derivatives have shown a peculiar behavior, making them different from the corresponding porphyrins, taken as reference macrocycles.[1] Corroles have demonstrated properties that can be of interest for applications in different fields, such as, for example, catalysis, photovoltaics, and chemical sensors, and these macrocycles can allow for dramatic improvements of device performances.[2] Preparatory to all these exploitations has been, of course, an optimization of synthetic procedures for the corrole preparation. For this reason, corrole-related research has experienced a dramatic explosion after the definition of simple synthetic routes for the preparation of *meso*-aryl substituted corroles.[3] Since then, different synthetic approaches have been proposed, which make the preparative scope of this macrocycles quite wide, comparable at least with the corresponding parent porphyrins.[4] In contrast to the progress achieved for the macrocycle preparation, a quite less developed field is the subsequent functionalization of corrole ring. This aspect is of fundamental importance for preparing organic materials, since a synthetic versatility is necessary to finely modulate the target properties by modification of the macrocycle. Some general examples reported in the literature have mostly focused on the halogenation and nitration reactions, taken as the first step for further functionalization of the corrole ring.[5] An exhaustive bromination of corrole, for example, has been used to prepare undecasubstituted corrole derivatives.[6] Among the different corrole functionalizations, we have been interested in the fusion of aromatic substituents at the macrocyclic β-positions. It is well-known that an expansion of the π-aromatic system of the macrocycle results in a remarkable modification of the optical features of the chromophore, which can be of interest for applications in photovoltaic derivatives, photodynamic therapy (PDT), or chemical sensors.[7] To reach this goal, Cavaleiro and co-workers tested the corrole reactivity in Diels–Alder cycloadditions, using 5,10,15-tris(pentafluorophenyl)corrole as dienophile in the reaction with pentacene.[8] The authors demonstrated how corroles can participate in Diels–Alder and in thermal [4 + 4] cycloadditions, revealing them to be even much more reactive than the porphyrin analogues under the same reaction conditions.

To test the scope of the Diels–Alder reaction with other corrole derivatives and with the aim to obtain a functionalized macrocycle, we studied the reaction between 5,10,15-tris(4-*tert*-butylphenyl)corrole **1** and 2,3-bis(bromomethyl)pyrazine **3**, following the procedure reported by Zhao and co-workers for *meso*-arylporphyrins.[9] However, it is well-known that corroles reveal in several cases an unpredictable reactivity, completely

Received: March 31, 2014
Published: June 30, 2014

   dx.doi.org/10.1021/ic500757a | *Inorg. Chem.* 2014, 53, 7404–7415

Scheme 1. Synthetic Pathway for the Formation of the 5-Hemiporphycene

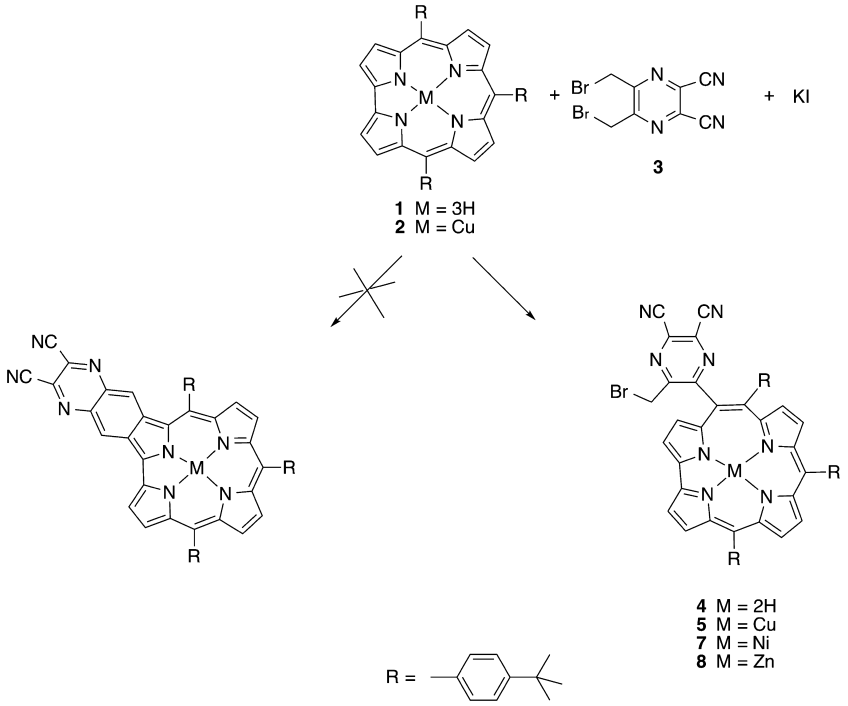

different from that of the corresponding porphyrins. Also, the product isolated in this case was not the expected corrole derivative, but a functionalized hemiporphycene, obtained by macrocyclic ring expansion (Scheme 1). This reactivity is not unprecedented in the case of corroles, because we have already reported the corrole-hemiporphycene conversion by reaction of the corrole with CI_4,[10] or by an analogous reaction with aminotriazole to obtain the corresponding azahemiporphycene derivative.[11] More recently Gross and co-workers have also reported a similar ring expansion to give 6-azahemiporphycene upon oxidation of a 5,10,15-tris(pentafluorophenyl)corrolato-Mn(III) complex.[12]

The results obtained demonstrate that this transformation of the corrole ring is not uncommon, and the scope of the reaction could be quite wide and interesting for the preparation of functionalized hemiporphycenes. We report here details of the reaction, together with spectroscopic and electrochemical characterization of the obtained hemiporphycene products.

EXPERIMENTAL SECTION

General Methods and Materials. Reagents and solvents (Sigma-Aldrich, Fluka and Carlo Erba Reagenti) were of synthetic grade and used without further purification. Silica gel 60 (70−230 mesh) was used for column chromatography. ^{1}H NMR spectra were recorded on a Bruker AV300 (300 MHz) spectrometer in $CDCl_3$ and in toluene-d_8. Chemical shifts are given in ppm relative to tetramethylsilane (TMS). NMR experiments ^{13}C, COSY, HSQC, HMBC, and ROESY were performed at T = 300 K on a Bruker Avance 600 MHz with a 5 mm inverse broadband probe equipped with z-axis gradients. UV−vis spectra were measured on a Varian Cary 50 spectrophotometer. Mass spectra were recorded on a VGQuattro spectrometer in the positive-ion mode, using m-nitrobenzyl alcohol (NBA, Aldrich) as a matrix (FAB).

Electrochemical and Spectroelectrochemical Measurements. Absolute dichloromethane (CH_2Cl_2, 99.8%, EMD Chemicals Inc.) was used for electrochemistry without further purification. Benzonitrile (PhCN), also used as a solvent for electrochemistry, was purchased from Sigma-Aldrich and distilled over P_2O_5 under a vacuum prior to use. Tetra-n-butylammonium perchlorate (TBAP), used as a supporting electrolyte, was purchased from Sigma-Aldrich, recrystallized from ethyl alcohol, and dried under a vacuum at 40 °C for at least 1 week prior to use.

Cyclic voltammetry was carried out with an EG&G model 173 potentiostat/galvanostat. A homemade three-electrode electrochemistry cell was used consisting of a platinum button or glassy carbon working electrode, a platinum wire counter electrode, and a saturated calomel reference electrode (SCE). The SCE was separated from the bulk of the solution by a fritted-glass bridge of low porosity which contained the solvent/supporting electrolyte mixture. All potentials are referenced to the SCE.

Thin-layer UV−visible spectroelectrochemical experiments were performed with a home-built thin-layer cell which has a light transparent platinum net working electrode. Potentials were applied and monitored with an EG&G model 173 potentiostat. Time-resolved UV−visible spectra were recorded with a Hewlett-Packard model 8453 diode array spectrophotometer. High purity N_2 from Trigas was used to deoxygenate the solution and kept over the solution during each electrochemical and spectroelectrochemical experiment.

SYNTHESES

Synthesis of 4 in Toluene. In a 100 mL round-bottomed flask, equipped with a stirring bar, 100 mg of 5,10,15-tris(4-*tert*-butylphenyl)corrole[13] **1** (0.144 mmol) was dissolved in 8 mL of toluene; **3** (182 mg; 0.576 mmol) and KI (96 mg; 0.576 mmol) were added, and the mixture was heated to reflux. The progress of the reaction was monitored by UV−vis spectroscopy and TLC. After the complete disappearing of the starting material, ca. 1 h, the solution was cooled to room temperature, and the solvent was evaporated under a vacuum. The crude product was purified by a column of silica gel using an eluting mixture of CH_2Cl_2/hexane (3:1) to isolate the unreacted **1** (17 mg, 0.025 mmol; 17%), traces of an inner core N-substituted corrole, and finally CH_2Cl_2 was used as eluant to obtained the desired 5-hemiporphycene **4** (16 mg, 0.017 mmol; 12%).

Synthesis of 4 in 1,2,4-Trichlorobenzene (TCB). In a 100 mL round-bottomed flask, equipped with a stirring bar, 100

dx.doi.org/10.1021/ic500757a | Inorg. Chem. 2014, 53, 7404−7415

mg of **1** (0.144 mmol) was dissolved in the minimum amount of TCB; **3** (182 mg; 0.576 mmol) and KI (96 mg; 0.576 mmol) were added, and the mixture was heated at the fixed temperature of 150 °C. The progress of the reaction was monitored by UV−vis spectroscopy and TLC. After the complete disappearing of starting material, ca. 30 min, the solution was cooled to room temperature, and the solvent was evaporated under a vacuum. The crude product was passed at first through a short plug of silica gel, to remove the decomposed material and subsequently purified by a column of silica gel eluting with a mixture of CH_2Cl_2/hexane (3:1) to isolate in order **6** (8 mg, 0.01 mmol, 7%), a mixture of Br-substituted 5-hemiporphycene (7 mg, 0.007 mmol; 5%) and the 5-hemiporphycene **4** (31 mg, 0.033; 23%).

5-Hemiporphycene 4. The brownish solid was recrystallized from CH_2Cl_2/methanol. Elem. Anal. Calcd for $C_{57}H_{51}BrN_8$: C, 73.77; H, 5.54; N, 12.07%. Found: C, 73.82; H, 5.59 N, 12.01%. UV−vis (CH_2Cl_2): λ_{max}, nm ($\varepsilon \times 10^{-3}$ L mol^{-1} cm^{-1}), 419 (74.1), 521 (6.0), 561 (8.1), 600 (3.89), 643 (7.8); ^{1}H NMR ($CDCl_3$): δ (ppm) 9.31 (1H, d, J = 4.4 Hz, β-pyrrole), 9.20 (1H, d, J = 4.4 Hz, β-pyrrole), 8.95 (1H, d, J = 4.4 Hz, β-pyrrole), 8.70 (1H, d, J = 4.5 Hz, β-pyrrole), 8.46 (1H, dd, J = 1.8 Hz; J = 2.7 Hz, β-pyrrole), 8.35 (1H, d, J = 4.7 Hz, β-pyrrole), 8.19 (2H, d, J = 7.2 Hz, o-Ph B), 8.15 (1H, d, J = 4.3 Hz, β-pyrrole), 8.09 (1H, dd, J = 2.1 Hz; J = 8.8 Hz, o-Ph A), 8.03 (1H, d, J = 4.8 Hz, β-pyrrole), 7.98 (1H, dd, J = 2.2 Hz; J = 8.8 Hz, o-Ph A), 7.86 (2H, d, J = 8.5 Hz, m-Ph B), 7.72 (1H, dd, J = 2 Hz; J 7.9 Hz, m-Ph A), 7.70 (1H, dd, J = 2 Hz; J = 7.9 Hz, m-Ph A), 7.51 (1H, d, J = 8 Hz, o-Ph C), 7.40 (1H, d, J = 8 Hz, o-Ph C), 7.51 (2H, brs, m-Ph C), 4.04 (1H, d, J = 10.8 Hz, −CH_2Br), 3.88 (1H, d, J = 10.8 Hz, −CH_2Br), 3.27 (2H, s, NH), 1.61 (9H, s, t-Bu B), 1.59 (9H, s, t-Bu A), 1.61 (9H, s, t-Bu C). ^{13}C NMR ($CDCl_3$): δ (ppm) 161.57−155.59 (C25−C26), 155.93−147.74 (C5−C6), 151.45 (C46), 151.17 (C34), 151.07 (C40), 148.45 (C17), 146.14 (C20), 144.36 (C15), 141.48 (C31), 140.75 (C37), 139.28 (C12), 135.95 (C9), 135.40 (C43), 135.15 (C16), 134.65 (C18), 134.54 (C4, C44−C48), 134.04 (C42), 133.38 (C38), 132.41 (C32), 132.00 (C8), 131.87 (C1), 130.79−129.53 (C28−C29), 130.35 (C13), 127.10−120.48 (C5−C6), 126.86 (C11), 126.72 (C14), 125.63 (C19), 125.49 (C3), 125.21 (C45−C47), 123.77 (C33−C35), 123.22 (C39), 123.20 (C41), 121.29 (C2), 113.01−112.71 (C28−C29), 34.96 (q t-Bu A, q t-Bu B), 34.79 (q t-Bu C), 31.65 (t-Bu B), 31.58 (t-Bu A), 31.37 (t-Bu C), 28.25 (CH_2Br). MS (FAB): isotopic clusters at m/z 928 ([M$^+$], 100%).

2-Br-*t*BuTPC 6. The light green solid was recrystallized from CH_2Cl_2/methanol. Anal. calcd for $C_{49}H_{49}BrN_4$: C, 76.05; H, 6.38; N, 7.24%. Found: C, 76.08; H, 6.41 N, 7.20%. UV−vis (CH_2Cl_2): λ_{max}, nm ($\varepsilon \times 10^{-3}$ L mol^{-1} cm^{-1}): 420 (100.0), 525 (sh), 567 (15.1), 617 (9.3), 661 (20.1); ^{1}H NMR δ_H ($CDCl_3$, J [Hz]) 9.22 ppm (1 H, d, J = 4.1, β-pyrrole), 8.96 (1 H, d, J = 4.6, β-pyrrole), 8.88 (1 H, d, J = 4.6, β-pyrrole), 8.72 (1 H, s, β-pyrrole), 8.58 (3 H, m, β-pyrrole), 8.42 (2 H, d, J = 8.0, phenyl), 8.22 (2 H, d, J = 8.0, phenyl), 8.13 (2 H, d, J = 7.9, phenyl), 7.89 (2 H, d, J = 8.0, phenyl), 7.81 (4 H, m, phenyl), 1.61 (27 H, br, s, *tert*-butyl); MS (FAB): isotopic clusters at m/z 774 ([M$^+$], 60%).

GENERAL PROCEDURE METAL COMPLEXES (M-4)

Cu, Ni, and Zn Complexes in CH_2Cl_2/MeOH. In a 50 mL round-bottomed flask, with a stirring bar, **4** (20 mg, 0.02 mmol) was dissolved in 10 mL of $CHCl_3$, and a saturated solution of $M(OAc)_2$ salt in methanol was added. The mixture was heated to reflux, and the progress of the reaction was followed by UV−vis spectroscopy and TLC. After disappearance of absorption peaks for the starting material, the solvent was evaporated under a vacuum, and the crude mixture was purified by chromatographic column.

Cu Complex 5. Purification of the reaction crude was performed on silica gel column eluting with CH_2Cl_2. The green fraction was recrystallized from CH_2Cl_2/methanol (14 mg; yield 68%). Elem. Anal. Calcd for $C_{57}H_{49}BrN_8Cu$: C, 69.19; H, 4.99; N, 11.32%. Found: C, 69.13; H, 4.94; N, 11.29%. UV−vis (CH_2Cl_2): λ_{max}, nm ($\varepsilon \times 10^{-3}$ L mol^{-1} cm^{-1}): 430 (85.1), 535 (4.0), 580 (5.4), 621 (22.4). MS (FAB): isotopic clusters at m/z 990 ([M$^+$], 100%).

Ni Complex 7. Purification of the reaction crude has been performed on silica gel column eluting with CH_2Cl_2. The green fraction was recrystallized from CH_2Cl_2/methanol (10 mg; yield 52%). Elem. Anal. Calcd for $C_{57}H_{49}BrN_8Ni$: C, 69.52; H, 5.02; N, 11.38%. Found: C, 69.49; H, 5.05; N, 11.42%. UV−vis (CH_2Cl_2): λ_{max}, nm ($\varepsilon \times 10^{-3}$ L mol^{-1} cm^{-1}): 411 (66.1), 618 (16.7), 653 (sh). ^{1}H NMR δ_H ($CDCl_3$, J [Hz]) 9.08 ppm (1 H, d, J = 4.7, β-pyrrole), 8.96 (1 H, d, J = 4.8, β-pyrrole), 8.79 (2 H, d, J = 4.8, β-pyrrole), 8.56 (1 H, d, J = 4.8, β-pyrrole), 8.44 (1 H, d, J = 5.0, β-pyrrole), 8.29 (1 H, d, J = 5.1, β-pyrrole), 8.10 (1 H, d, J = 4.6, β-pyrrole), 8.00 (3 H, m, phenyl), 7.78 (3 H, d, J = 8.1, phenyl), 7.65 (4 H, m, phenyl), 7.41 (1 H, m, phenyl), 6.93 (1 H, m, phenyl), 3.73 (1 H, d, J = 10.8, −CH_2Br), 3.38 (1 H, d, J = 10.8, −CH_2Br), 1.61 (18 H, s, *tert*-butyl), 1.40 (9 H, s, *tert*-butyl); MS (FAB): isotopic clusters at m/z 985 ([M$^+$], 80%).

Zn Complex 8. Purification of the reaction crude has been performed on silica gel column eluting with CH_2Cl_2. The green fraction was recrystallized from CH_2Cl_2/methanol (17 mg; yield 84%). Elem. Anal. Calcd for $C_{57}H_{49}BrN_8Zn$: C, 69.06; H, 4.98; N, 11.30%. Found: C, 69.11; H, 4.95 N, 11.22%. UV−vis (CH_2Cl_2): λ_{max}, nm ($\varepsilon \times 10^{-3}$ L mol^{-1} cm^{-1}): 433 (53.7), 538 (2.7), 581 (3.5), 615 (sh), 631 (13.8). ^{1}H NMR δ_H ($CDCl_3$, J [Hz]) 9.27 ppm (1 H, d, J = 4.1, β-pyrrole), 9.21 (1 H, d, J = 4.2, β-pyrrole), 9.02 (1 H, d, J = 4.0, β-pyrrole), 8.89 (1 H, d, J = 4.5, β-pyrrole), 8.64 (2 H, m, β-pyrrole), 8.38 (1 H, d, J = 4.6, β-pyrrole), 8.14 (3 H, m, β-pyrrole + phenyl), 8.00 (1 H, d, J = 7.6, phenyl), 7.84 (2 H, d, J = 8.2, phenyl), 7.72 (2 H, m, phenyl), 7.55 (1 H, m, phenyl), 7.50 (1 H, m, phenyl), 7.49 (1 H, m, phenyl), 7.43 (2 H, d, J = 7.4, phenyl), 7.35 (1 H, m, phenyl), 4.08 (1 H, d, J = 10.8, −CH_2Br), 3.95 (1 H, d, J = 11.1, −CH_2Br), 1.63 (9 H, s, *tert*-butyl), 1.60 (9 H, s, *tert*-butyl), 1.47 (9 H, s, *tert*-butyl); MS (FAB): isotopic clusters at m/z 991 ([M$^+$], 90%).

Ni Complex in DMF. In a 50 mL round-bottomed flask, with a stirring bar, **4** (20 mg, 0.02 mmol) was dissolved in 8 mL of DMF, and 3-fold excess of $NiCl_2$ salt was added. The mixture was heated to reflux, and the progress of the reaction was followed by UV−vis spectroscopy and TLC. After disappearance of absorption peaks for the starting material, the solvent was evaporated under a vacuum, and the crude mixture was purified by chromatography on neutral alumina using $CHCl_3$/hexane (1:1) as the eluent.

Ni Complex 9. Purification of the reaction crude has been performed on silica gel column eluting with CH_2Cl_2. The green fraction was recrystallized from CH_2Cl_2/methanol (9 mg; yield 47%). Elem. Anal. Calcd for $C_{57}H_{50}N_8Ni$: C, 75.58; H, 5.56; N, 12.37%. Found: C, 75.44; H, 5.80 N, 12.32%. UV−vis (CH_2Cl_2): λ_{max}, nm ($\varepsilon \times 10^{-3}$ L mol^{-1} cm^{-1}): 409 (87.1), 456 (sh), 617 (23.4), 656 (sh). ^{1}H NMR δ_H ($CDCl_3$, J [Hz])

dx.doi.org/10.1021/ic500757a | Inorg. Chem. 2014, 53, 7404−7415

9.03 ppm (1 H, d, J = 4.5, β-pyrrole), 8.93 (1 H, d, J = 4.8, β-pyrrole), 8.76 (2 H, m, β-pyrrole), 8.53 (1 H, d, J = 4.8, β-pyrrole), 8.42 (1 H, d, J = 5.0, β-pyrrole), 8.27 (1 H, d, J = 5.1, β-pyrrole), 8.13 (3 H, br, phenyl), 8.00 (2 H, m, phenyl), 7.93 (1 H, d, J = 4.6, β-pyrrole), 7.77 (3 H, d, J = 8.4, phenyl), 7.64 (3 H, br, phenyl), 7.44 (1 H, br, phenyl), 7.21 (1 H, br, phenyl), 6.91 (1 H, br, phenyl), 1.73 (3 H, s, $-CH_2Br$), 1.59 (18 H, s, *tert*-butyl), 1.40 (9 H, s, *tert*-butyl); isotopic clusters at m/z 907 ([M^+], 100%).

RESULTS AND DISCUSSION

The objective of our study was initially the preparation of corroles having an extended π-system, using corrole as substrate in a Diels–Alder reaction, following the same approach exploited by Zhao and co-workers for *meso*-tetrarylporphyrins.[9] We decided to carry out the reaction on 5,10,15-tris(4-*tert*-butylphenyl)corrolato copper **2**, taking advantage of the higher stability of the copper complex than the corresponding corrole free-base.

Complex **2** was reacted with pyrazine *o*-quinodimethane, generated in situ from the corresponding 2,3-bis-(bromomethyl)pyrazine derivative **3**, in the presence of KI, and the mixture was heated to reflux in TCB. After 1 h, no starting material was present in the TLC control of the reaction progress, while, in the meantime, some polar products were evidenced. The reaction work up and the subsequent chromatographic separation afforded two major fractions; the UV–vis spectra of both samples suggested them as being copper complexes, although the corresponding ^{1}H NMR analysis showed a paramagnetic nature, which is unusual for Cu corroles. To avoid this problem, we decided to repeat the same reaction on the corresponding free-base **1**. In this case, the reaction was complete after 20 min, and a major product was isolated, while a second fraction was obtained in trace amounts. A significant amount of decomposed material was observed. The major fraction was characterized as a hemiporphycene derivative, where the pyrazine fragment was inserted at a *meso*-position of the macrocycle, according to the spectroscopic characterization. Other than the hemiporphycene-like UV–vis spectrum, the IR spectrum showed the bands of CN groups, and the ^{1}H NMR showed the presence of sharp and separate β-pyrrolic signals and two doublets, with high coupling constants, around 4 ppm, corresponding to the nonequivalent CH_2 protons of the (bromomethyl)pyrazine group; finally the mass spectrum showed the molecular peak together with an isotope pattern of signals characteristic of bromine.

The formation of a hemiporphycene derivative is a further example of the corrole ring "breathing", which can expand, affording different porphyrinoids, such as porphyrins,[14] azaporphyrins,[15] hemiporphycenes,[10] and azahemiporphycenes,[11,12] depending on the reaction conditions.[16]

However, in this last case, the regioselectivity of the reaction should be defined; in previous studies we observed that ring insertion leads to a 5-substituted species in the case of hemiporphycene, while the corresponding aza-derivative was revealed to be a 6-azahemiporphycene.

Unfortunately, all attempts to grow single crystals of **4** for X-ray characterization have been unsuccessful, and, for this reason, a ^{1}H NMR study was attempted to characterize the obtained hemiporphycene. Again this corrole metamorphosis involves a breaking of the bond between carbon 4 and the *meso* carbon 5, leading to the formation of a 5-substituted hemiporphycene (Figure 1), as unambiguously identified by means of concerted NMR experiments (^{1}H, ^{13}C, COSY, HSQC, HMBC, and ROESY, Figures S1–S6, Supporting Information), which allowed an assignment for all resonances in the ^{1}H and ^{13}C NMR spectra. The insertion of a carbon atom within the macrocycle introduces a strong asymmetry in the whole molecule, thus inducing the splitting of each proton and carbon resonance in the ^{1}H and ^{13}C NMR spectra. The complete list of proton and carbon chemical shifts is reported in Table 1.

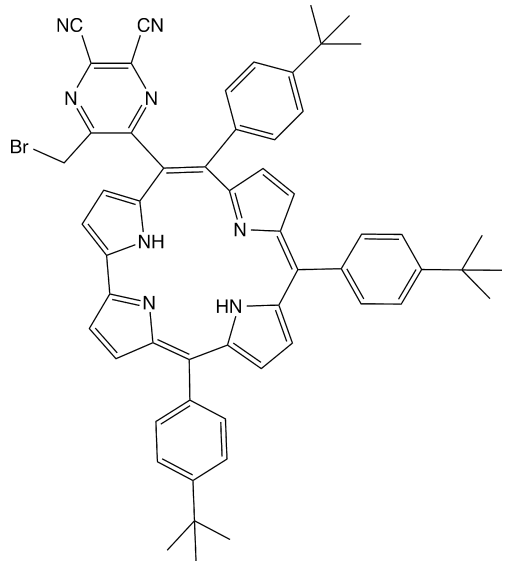

Figure 1. Structure of hemiporphycene as deduced by concerted NMR experiments.

As a result of the loss of symmetry, eight doublets between 9.4 and 7.9 ppm were observed in the ^{1}H NMR spectrum, one for each β-pyrrolic proton. The coupling pattern of each pair of β-pyrrolic protons was readily observed in the COSY spectrum (see Figure S3). Furthermore, the distortion of the macrocycle provides extremely different rotational freedom for the three different phenyl rings (named "A", "B", and "C"). In the low temperature ^{1}H NMR (262 K) reported in Figure S2, all the *ortho* protons (the position *ortho* is intended with respect to the macrocycle) are split into two different resonances, reflecting two different orientations toward the nonsymmetrical plane of the molecule. As the temperature is increased, the rotational barriers can be overcome, and *ortho* protons give rise to a single signal. This is the case of the *ortho* protons of phenyl B at 300 K (see Figure S1), whereas those of phenyl C are close to coalescence. Instead, the *ortho* protons of phenyl A are still split apart. Such a peculiar T dependence points out an unexpected order in the rotational freedom of phenyl rings: B > C $\gg$ A. However, this interesting conformational aspect deserves further examination and will be a subject of future studies.

A ROESY experiment was used (see Figure 2B–C) to determine whether the insertion of the pyrazine ring occurred at position 5 or 6. First of all the relatively strong cross peaks observed between H(2) and H(19) allowed for an unequivocal assignment of the chemical shifts. Starting from this information, every resonance was assigned. The most relevant dipolar couplings are highlighted in Figure 2A and provided the relative positions of each phenyl ring: phenyl A is in between

dx.doi.org/10.1021/ic500757a | Inorg. Chem. 2014, 53, 7404–7415

Table 1. ^{1}H and ^{13}C Observed Chemical Shifts for Compound 4

position	δ ^{1}H (ppm)	δ ^{13}C (ppm)
1		131.87
2	9.31	121.29
3	8.15	125.49
4		134.54
5; 6		127.10−120.48[a]
7; 10		147.74−155.93[a]
8	8.03	132.00
9	8.35	135.95
11		126.86
12		139.28
13	8.46	130.35
14	8.70	126.72
15		144.36
16		135.15
17		148.44
18	8.95	134.65
19	9.20	125.63
20		146.14
NH	3.27	
-CH_2Br	3.88	28.25
-CH_2Br	4.04	28.25
25; 26		155.59−161.57[a]
28; 29		129.53−130.79[a]
28-CN; 29-CN		112.71−113.01[a]
31		141.48
32	7.51	132.41
33−35	7.39	123.77
34		151.17
36	7.40	132.41
t-Bu (q)		34.79
t-Bu	1.44	31.37
37		140.75
38	8.09	133.38
39	7.72	123.22
40		151.07
41	7.70	123.20
42	7.98	134.04
t-Bu (q)		34.96
t-Bu	1.59	31.58
43		135.40
44−48	8.19	134.54
45−47	7.86	125.21
46		151.45
t-Bu (q)		34.96
t-Bu	1.61	31.65

[a]Chemical shifts might be inverted.

H(9) and H(13); phenyl B is in between H(14) and H(18); and phenyl C is close to the pyrazinyl group.

Most importantly, the protons of the peripheral CH_2Br group of the pyrazinyl moiety are close in space to both the ortho protons of the phenyl C and to H(3) (see Figure 2B). Such a pattern is expected if the substituent was inserted at the position 5. Conversely, if the insertion of the pyrazinyl group occurred at the position 6, a dipolar coupling between the peripheral CH_2 protons and H(8) would be expected. Therefore, the insertion was unequivocally assigned at position 5. Since C protons are well observable only at low temperature, ROESY spectra were carried out at about 260 K. It is worth noting that the CH_2 protons appear as two doublets in the whole range of temperature explored (262−310 K), thus reflecting a high rotational barrier of the pyrazinyl ring. Interestingly, the blockage of the latter allows for free rotation of the neighboring phenyl C above 310 K.

Prompted by this interesting result, we decide to optimize the reaction conditions, by changing different parameters, such as temperature, solvent, or reagents molar ratio, with the aim to characterize also the fraction observed in traces.

The reduction of the reaction temperature was effective, since a significant reduction of the decomposition products was observed; however, a good compromise should be obtained, since if the temperature is too low, the activation of 2,3-bis(bromomethyl)pyrazine by KI is not complete, making the reaction not possible. The highest yields of hemiporphycene were obtained when carrying out the reaction at 150 °C in TCB, and significant improvements came also from reduction of the excess KI, which resulted in a decrease of decomposition byproducts. The best results were obtained using a 1:1 molar ratio of KI and pyrazine, in 4-fold excess with respect to corrole. Under these conditions, other than the 5-hemiporpycene **4**, a chromatographic purification of the reaction mixture afforded two additional products, corresponding respectively to 2-bromo corrole **6** and a mixture of mono bromo-hemiporphycenes (Scheme 2).

Some hypothesis can be proposed for the formation of these brominated products; it is well-known that corroles can be easily oxidized, which is one of the reasons for the corrole liability. In the reaction condition utilized, it is reasonable that corrole could be oxidized, forming a π-cation radical species; this species can be attacked by nucleophiles, leading to β-substituted species, as we have recently reported.[13,17,18] Since Br^- ion is present in the reaction mixture, from the activation of the pyrazino precursor, it is reasonable to hypothesize that it is the result of the corrole oxidation, followed by the Br addition. On the other hand, we observed also the evolution of I_2 from the reaction, a reagent that has been used for oxidative β-corrole functionalization.[13]

This hypothesis was confirmed by observing that the reaction also worked when the corresponding isocorroles are used as starting materials. These oxidized forms of corroles can form radicalic species by thermal treatment and then undergo the ring expansion to give hemiporphycene derivatives. Further support to this hypothesis is given by the observation that 5-isocorrole and 10-isocorrole afforded the same 5-hemiporphycene, according to their formation of the same π-cation radical of corrole.

It is plausible to believe that the 2-Br corrole can undergo the ring expansion, leading to the final mixture of bromohemiporphycenes, which should lead to formation of a mixture of 2-Br- and 19-Br-5-hemiporphycenes. A mono substitution is indicated by the mass spectrum of these products. However, we cannot exclude the alternative hypothesis featuring a bromination of the formed hemiporphycene; the low amount of these products and the almost identical chromatographic R_f precluded separation of these isomers and their complete characterization.

A completely different behavior is observed when carrying out the reaction in a different solvent such as toluene. In this case a complete conversion of the starting corrole is not achieved, and the products are a mixture of the expected 5-hemiporphycene **4** and traces of an additional corrole, while no brominated products are observed under these conditions. The

dx.doi.org/10.1021/ic500757a | Inorg. Chem. 2014, 53, 7404−7415

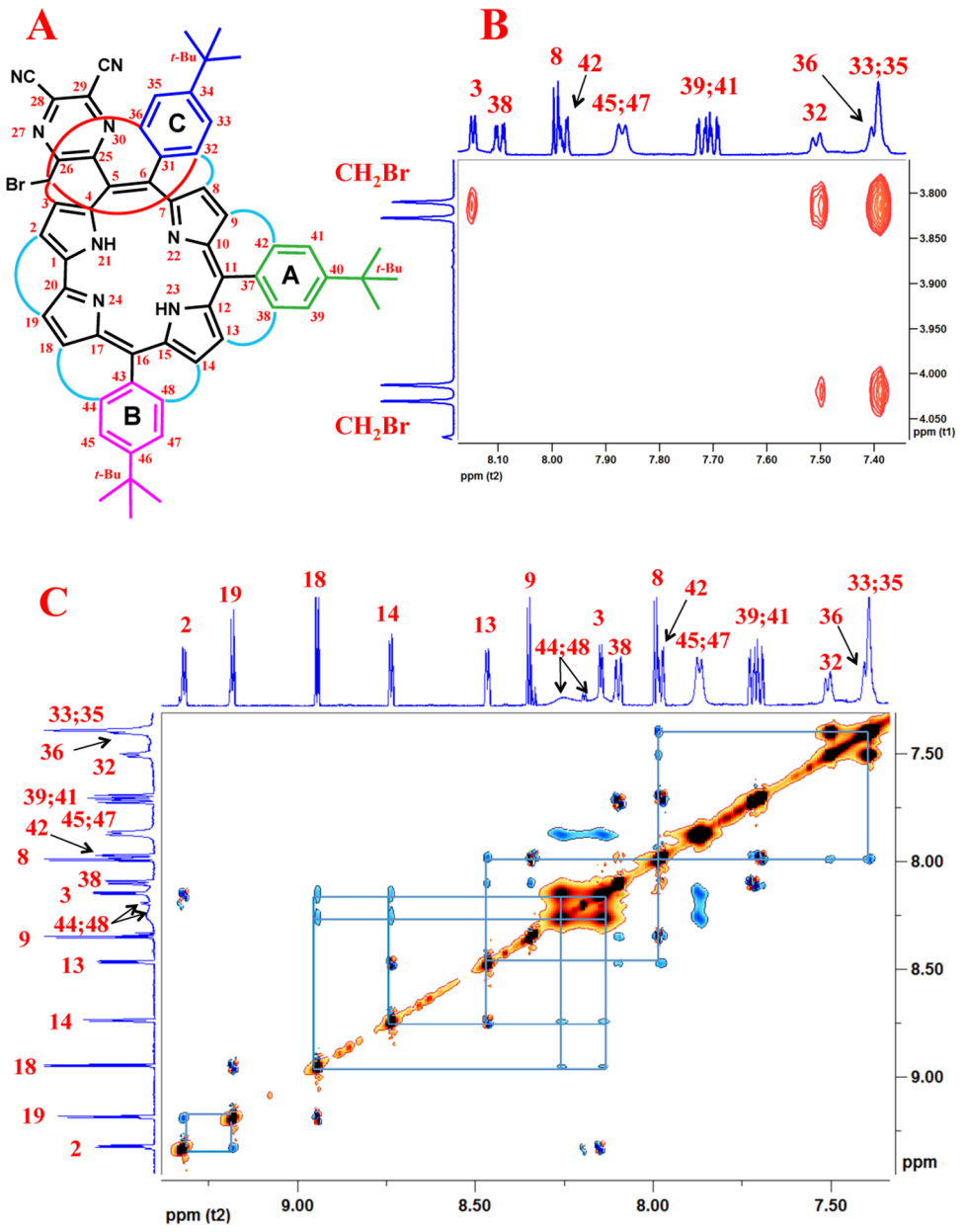

Figure 2. Structure of hemiporphycene **4** with connectivities (A) which points out the dipolar coupling observed in the ROESY spectra ($CDCl_3$, 262 K) reported in (B) and (C). Red lines refer to dipolar couplings observed in (B), while cyano lines refer to that observed in (C).

mass spectrum of the trace byproduct exhibits a molecular peak at 851 *m*/*z*, without the isotopic pattern of a bromine atom. The ^{1}H NMR spectrum showed an asymmetric substitution pattern, with eight doublets of the *β*-pyrrolic protons. These results strongly suggest formation of an inner core substituted corrole, with the pyrazino group bridged among two nitrogen atoms of the corrole core. Unfortunately this compound can only be separated in trace amounts by thin layer chromatography, and this prevented its complete characterization.

Formation of the brominated products is not seen in toluene, probably due to the milder reaction conditions, but, on the other hand, we also observed an incomplete corrole conversion, which can be recovered at the end of reaction, reducing the final yields. It is also worth mentioning that the reaction was not successful in more polar solvents, and only a decomposition of the starting corrole was observed to occur.

FORMATION OF METAL COMPLEXES

We wished to investigate the coordination ability of the functionalized 5-hemiporphycenes since the *meso*-pyrazino ring is potentially interesting for future additional modifications of the hemiporphycene ring. However, it should be noted that the peripheral pyrazine substituent can strongly influence the properties of the macrocycle, since this group can react under the metalation reaction conditions usually adopted for analogous porphyrin derivatives. The currently investigated porphyrinoids show much weaker coordination properties than the previously studied analogous 6-azahemiporphycenes. Nonetheless, we were able to obtain metal complexes of Zn(II), Cu(II), and Ni(II), although decomposition was observed when attempting to obtain complexes with trivalent metal ions, such as Fe(III) or Mn(III). This result is probably due to a reaction of the *meso*-pyrazino substituent under the utilized reaction conditions.

dx.doi.org/10.1021/ic500757a | *Inorg. Chem.* 2014, 53, 7404−7415

Scheme 2

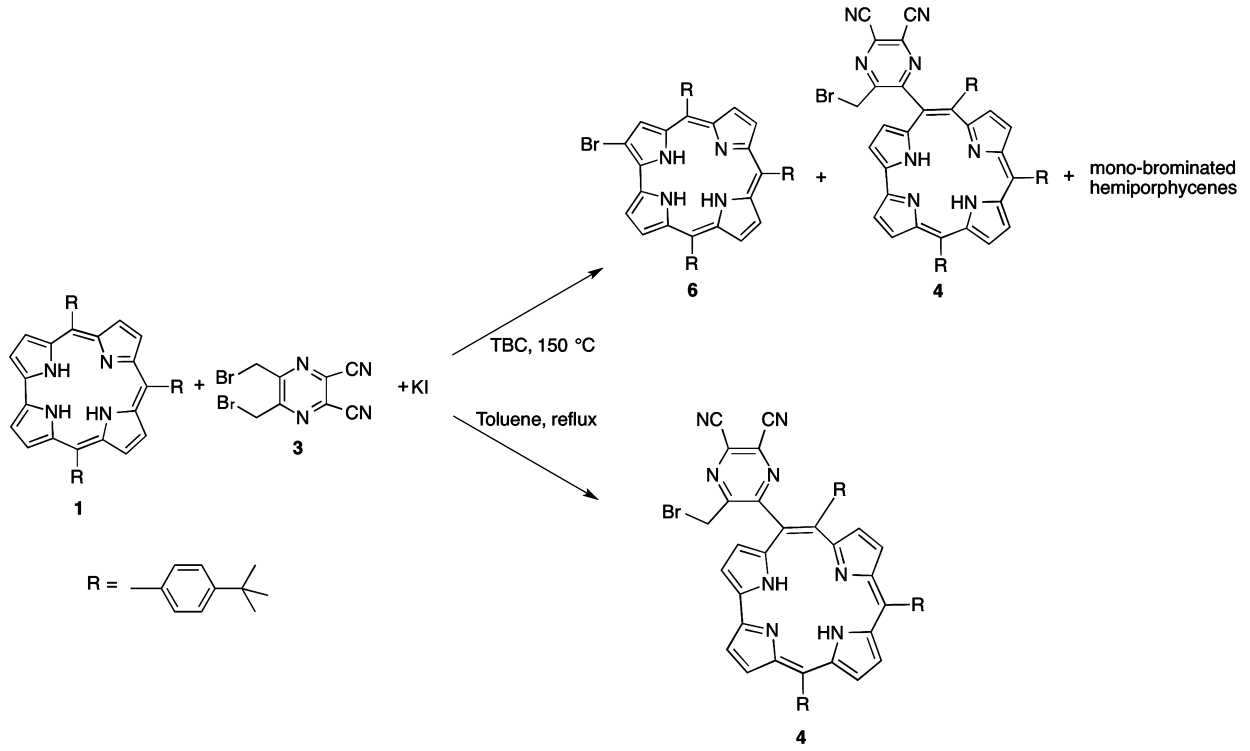

Table 2

solvent	reagents ratio[a] 1:3:KI	T (°C)	yield (%)
TCB	1:10:30	reflux	6
toluene	1:10:30	reflux	10
toluene	1:5:10	reflux	12
TCB	1:5:10	150	16
TCB	1:4:4	150	23
TCB	1:3:3	150	14

[a]Pyrazine **3** and KI amounts are expressed as equivalents vs corrole 1 mol.

This hypothesis was confirmed in the case of the Ni complex. Because the metalation reaction was not complete after 25 h, when carried out in a mixed CH_2Cl_2/MeOH solvent, we decided to carry out the reaction in DMF, which is usually successful in the metalation of porphyrins. In this case we were able to obtain good yields of a Ni hemiporphycene, but characterization of the complex indicated that the isolated product was actually the debrominated species **9** shown in Figure 3.

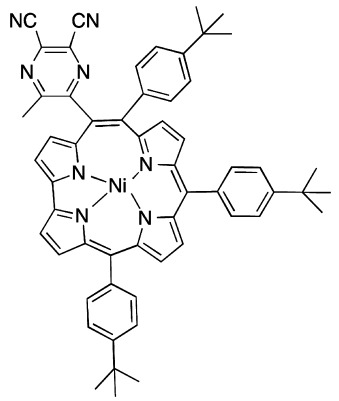

Figure 3. Structure of the complex **9** synthesized in DMF.

ELECTROCHEMISTRY

To further investigate the isolated products, the 5-hemiporphycene derivatives were examined by cyclic voltammetry and thin-layer spectroelectrochemistry in dichloromethane (CH_2Cl_2) and benzonitrile (PhCN) containing 0.1 M tetra-*n*-butylammonium perchlorate (TBAP) as supporting electrolyte. Examples of the cyclic voltammograms in CH_2Cl_2 are illustrated in Figure 4, and a summary of the half-wave or peak potentials in CH_2Cl_2 and PhCN is given in Table 3, which also indicates the proposed site of each electron transfer.

The investigated compounds possess two electroactive redox centers; one is the conjugated π-ring system of the hemiporphycene macrocycle and the other is the linked pyrazine group, which shows a rich redox activity upon reduction. As described on the following pages, the hemiporphycene complex undergoes two macrocycle-centered oxidations and one or two macrocycle-centered reductions, the remaining redox processes being assigned to reductions at the pyrazine substituent. Evidence for electron addition to the pyrazine substituent on these complexes is given by data in the literature for a variety of substituted pyrazines with electron withdrawing groups[19] and by an examination in the present study of the pyrazines **3** and **10** in PhCN (see Chart 1).

Pyrazine and substituted pyrazines have been shown to undergo up to two one-electron reductions in nonaqueous solvents such as CH_2Cl_2, PhCN, and pyridine.[10] The potentials and reversibility of these reactions will depend upon the specific pyrazine substituents. One example related to the current study is **10**, which is reversibly reduced in PhCN at $E_{1/2} = -0.93$ V in the first step and irreversibly reduced at $E_p = -1.82$ V in the second (see Table 3). The potential separation between the two reductions of **10** in PhCN amounts to 890 mV, and this

dx.doi.org/10.1021/ic500757a | Inorg. Chem. 2014, 53, 7404−7415

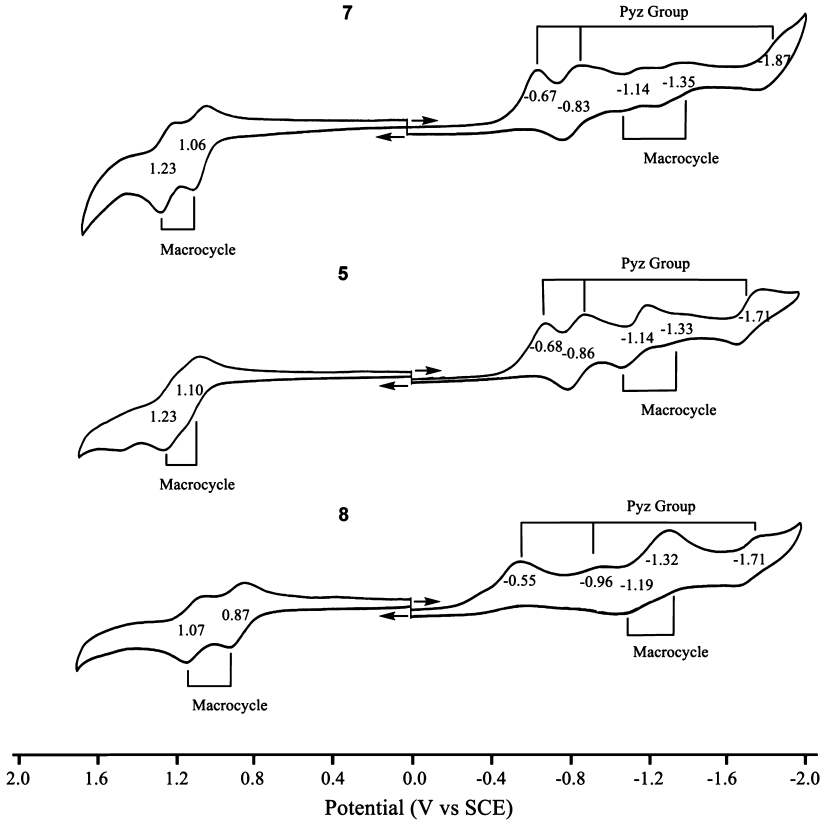

Figure 4. Cyclic voltammograms of complexes **5**, **7**, and **8** in CH_2Cl_2 containing 0.1 M TBAP.

Table 3. Half-Wave Potentials (V vs SCE) of Hemiporphycenes and Related Small Molecules in CH_2Cl_2 or PhCN Containing 0.1 M TBAP

		hemiporphycene macrocycle				pyrazine group		
		oxidation		reduction		reduction		
solvent	compound/pyrazine[a]	second	first	first	second	first	second	third
CH_2Cl_2	**4**	1.39	1.18[a]	−1.18	−1.51[a]	−0.68[a]	−0.82	−1.59
	9	1.27	1.08	−1.18[a]			−0.81	−1.77
	7	1.23	1.06	−1.14	−1.35	−0.67[a]	−0.83	−1.87
	5	1.23	1.10	−1.14	−1.33	−0.68[a]	−0.86	−1.71
	8	1.07	0.87	−1.19	−1.32	−0.55[a]	−0.96[a]	−1.71
	3					−0.56[a]		
PhCN	**4**	1.36	1.16[a]	−1.20	−1.47	−0.66[a]	−0.82	−1.47
	9	1.27	1.12	−1.14[a]			−0.85	−1.69
	7	1.25	1.12	−1.18[a]	−1.37	−0.67[a]	−0.83	−1.68
	5	1.29	1.13	−1.18	−1.36	−0.68[a]	−0.85	−1.70
	8	1.13	0.95	−1.19	−1.28	−0.60[a]	−1.00[a]	−1.74
	3					−0.55[a]		
	10						−0.93	−1.82[a]

[a]Irreversible peak potential at scan rate of 0.1 V/s.

Chart 1

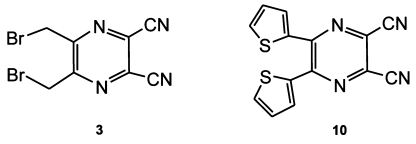

value can be compared to a separation of 750−1040 mV between the second and fifth reductions of the four investigated hemiporphycene complexes in the same solvent. A similar separation is seen in CH_2Cl_2, and these processes are labeled in Figure 4 as occurring at the pyrazine group for complexes **5**, **7**, and **8**.

The first one-electron reduction of **4** and the complexes **5**, **7**, and **8** in Figure 4 at E_p = −0.55 to −0.68 V is also proposed to occur at the pyrazine group, but this electron transfer is irreversible and accompanied by a loss of Br^-, with the conversion to the debrominated species in solution. Evidence for this assignment is given in part by the cyclic voltammograms in Figure 5 for the reduction of **3** in PhCN. The first one-electron addition to this compound at E_p = −0.55 V is irreversible and coupled to an oxidation peak at E_p = 0.76 V,

dx.doi.org/10.1021/ic500757a | Inorg. Chem. 2014, 53, 7404−7415

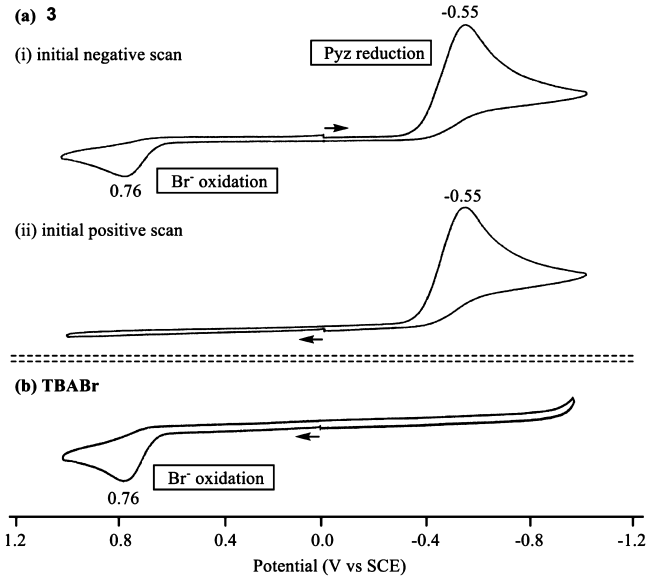

Figure 5. Cyclic voltammograms of (a) **3** ($c = 1.1 \times 10^{-4}$ M) and (b) TBABr ($c = 1.0 \times 10^{-4}$ M) in PhCN, 0.1 M TBAP.

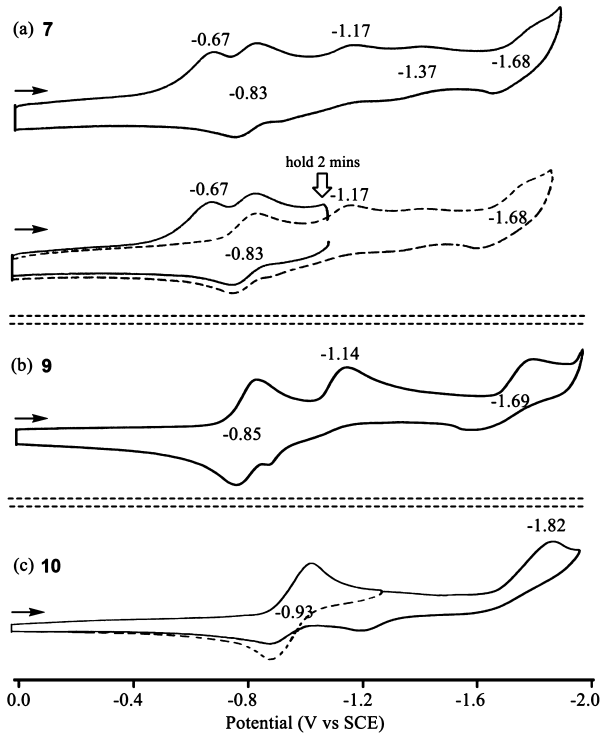

Figure 6. Cyclic voltammograms of (a) **7**, (b) **9**, and (c) **10** in PhCN, 0.1 M TBAP.

which is not seen upon an initial positive scan (Figure 5a). A similar oxidation peak is observed at $E_p = 0.76$ V for a PhCN solution of tetra-*n*-butylammonium bromide (TBABr) (Figure 5b). In both cases, this peak is assigned to the oxidation of Br^-, either from TBABr or from bromide, which is in situ generated after the first one-electron reduction of **3**.

Like in the case of **3**, the first one-electron reduction of **4**, **5**, **7**, and **8** is irreversible and coupled with a new oxidation peak at 0.78 V, which is not seen on initial positive scans of the compounds (see Figure 4). The hemiporphycene product of the chemical reaction following the first reduction is the unreduced hemiporphycene, which has lost a Br substituent from the pyrazine group and added in its place a proton from the solution. This debrominated pyrazine substituent is then the site of the second one-electron reduction in the cyclic voltammograms of these compounds. This pyrazine-based reduction is reversible for three of the four hemiporphycene derivatives and located at a similar half-wave potential of −0.81 to −0.86 V, independent of the solvent or central metal ion. A comparable reversible reduction is also seen in PhCN at $E_{1/2}$ = −0.82 V for **4** and at $E_{1/2}$ = −0.96 V for **3** (see Table 3).

Additional electrochemical evidence for pyrazine being the site of the second reduction is given by a comparison of the cyclic voltammograms for the reduction of the Ni complexes **7** and **9**. As described above, the first reduction of **9** is proposed to generate a neutral hemiporphycene with a debrominated pyrazine group. The debrominated Ni complex (**9**, Figure 3) was chemically synthesized as described in the Experimental Section and exhibits redox behavior almost identical to that of **7**, after the first irreversible reduction of this compound. This is most clearly seen on the second potential scan in the cyclic voltammogram of **7**, where the process at $E_p = -0.67$ V is no longer present (dashed line in Figure 6a). The third (and last) reduction of **9** (Figure 6b) at $E_{1/2} = -1.69$ V is assigned to the second reduction of the pyrazine group, and a similar redox process is seen for **10** in Figure 6c.

The electrochemistry of **5** is quite similar to that of **7**, both in the number of observed electrochemical reactions and in the measured redox potentials. For both compounds, the first, second and fifth reductions are assigned to the pyrazine group, while the third and fourth reductions are assigned as electron addition to the conjugated macrocycle of the hemiporphycene.

This assignment of electron transfer site in the first four reductions was further verified for **5** by monitoring the UV−visible spectral changes during controlled potential reduction in a thin-layer cell. These results are illustrated in Figure 7. As seen in the figure, the first two one-electron reductions at controlled potentials of −0.80 and −1.00 V exhibit negligible spectral changes, consistent with electron addition to the pyrazine group which does not interact substantially with the π-ring system of the hemiporphycene macrocycle. In contrast, a controlled potential reduction at −1.60 V directly effects the π-ring system of the hemiporphycene. The spectral changes and the final UV−visible spectrum are characteristic of electron addition to the conjugated macrocycle and formation of a hemiporphycene π-anion radical in the first step. These spectral changes are illustrated at the bottom of Figure 7.

Hemiporphycene Oxidations and HOMO−LUMO Gap. Each investigated metal hemiporphycene complex undergoes two well-defined ring centered one-electron oxidations. The first is located at $E_{1/2}$ = 0.87 to 1.10 V, and the second at $E_{1/2}$ values between 1.07 to 1.39 V in CH_2Cl_2 containing 0.1 M TBAP (see Table 3 and Figure 4). The first oxidation of **4** is irreversible in both solvents, probably due to a protonation reaction of the free-base hemiporphycene.[20]

No differences in the first oxidation potentials are seen between **7** and **9** in PhCN, indicating the lack of a substituent effect for the Br group on the pyrazine. A similar lack of substituent effect is seen for the second oxidation which differs by 0−20 mV between the two compounds in PhCN or CH_2Cl_2. No pyrazine-centered oxidations are observed, either for the investigated hemiporphycenes or for the two substituted dicyanopyrazine molecules examined in the current study.

dx.doi.org/10.1021/ic500757a | Inorg. Chem. 2014, 53, 7404−7415

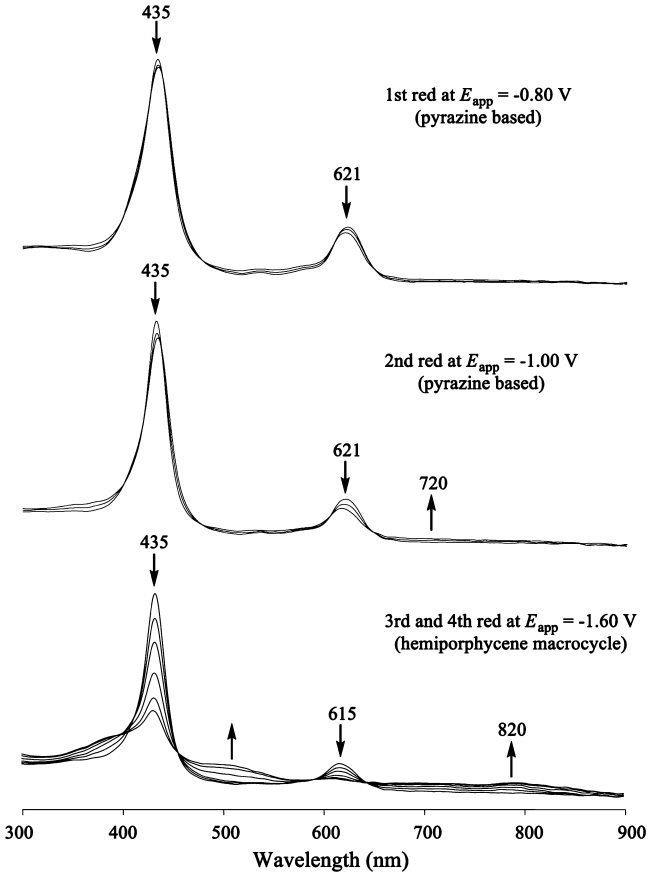

Figure 7. UV−visible spectral change during controlled potential reduction of **5** in PhCN, 0.1 M TBAP at the indicated potentials.

Spectroscopic support for assignment of the two reversible oxidations of the complexes as involving the hemiporphycene π-ring system is given by the thin-layer spectroelectrochemistry data shown in Figure 8a for the case of **5**. Controlled potential oxidation at 1.20 V leads to a spectrum with decreased intensity of the Soret and Q bands, as a broad new band grows in between 700 and 900 nm for the singly oxidized compound. This type of spectral change indicates a one-electron abstraction from the hemiporphycene macrocycle and produces a typical π-cation radical type spectrum as the final electro-oxidation product. Similar spectral changes are observed for **7** and **8** complexes during the first oxidation. The second oxidation of **5** at 1.70 V leads to a complete loss of intensity for all bands, consistent with formation of a hemiporphycene dication (Figure 8a).

A different type of spectral change is observed upon oxidation of the free-base hemiporphycene **4** (Figure 8b) in PhCN. The first oxidation is irreversible by cyclic voltammogram and applying a controlled oxidation potential of 1.30 V to **4** in a thin-layer cell results in a decrease of the original Soret band peak at 423 nm, with the apperance of a new Soret band at 452 nm. A new relatively intense Q-band also forms at 696 nm for the singly oxidized species. These types of spectral changes can be interpreted in terms of a fast protonation reaction at the central nitrogen to give the diprotonated neutral hemiporphycene, $[\mathbf{4}]^{2+}$ (see Figure 8b).[20]

The electrochemically measured HOMO−LUMO gap (the difference in $E_{1/2}$ of the first ring-centered oxidation and reduction) for **4** and **5**, **7**, **8** complexes also supports our assignents for oxidation and reduction at the π-ring system of the hemiporphycene macrocycle. The potential for the first oxidation and first reduction of **5**, **7**, **8** and the corresponding tetraphenylporphyrin complexes (TPP)M[21] are graphically shown in Figure 9. As seen in the figure, the first oxidation of hemiporphycene complexes (TPHpBr)M is systematically harder than the first oxidation of the corresponding (TPP)M compounds by 50−70 mV. At the same time, the difference in $E_{1/2}$ between reduction of (TPHpBr)M and (TPP)M ranges from 140 to 180 mV, with the most facile reduction occurring for the hemiporphycene macrocycle. The easier reduction of the hemiporphycenes results in a smaller HOMO−LUMO gap

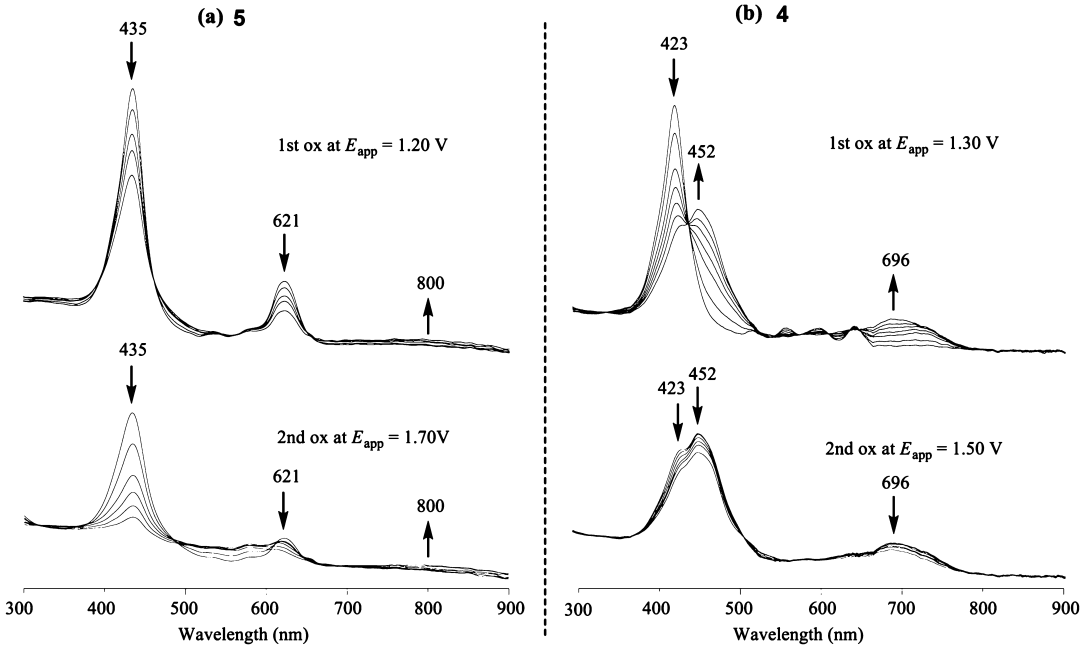

Figure 8. UV−visible spectral change during the controlled potential oxidations of (a) **5** and (b) **4** in PhCN, 0.1 M TBAP.

dx.doi.org/10.1021/ic500757a | *Inorg. Chem.* 2014, 53, 7404−7415

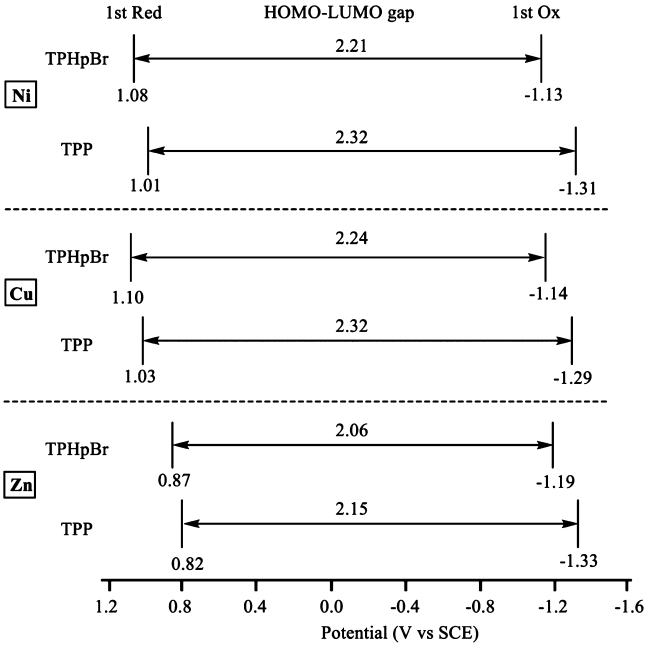

Figure 9. Comparison of redox potentials for first oxidation and first reduction of (TPHpBr)M and (TPP)M where M = Ni, Cu, or Zn.

for these compounds as compared to the (TPP)M derivatives by 80−110 mV, and the values of the gap that ranges from 2.06 to 2.24 V for (TPHpBr)M are shown in Figure 9.

CONCLUSIONS

The formation of the 5-hemiporphycene **4** represents a further example of corrole ring "breathing" and demonstrates that this transformation is not unusual, but it can be of synthetic value for the preparation of functionalized species of this porphyrin analogue, considering the significant developments recently achieved by the synthetic chemistry of corrole. The oxidation of corrole is probably the first step of the reaction, since the reaction proceeds also if the starting material is an isocorrole. Different metal complexes of 5-hemiporphycene have been prepared, and the electrochemistry of these compounds reveal the reactivity of the peripheral pyrazino group. The singly reduced products undergo the loss of a Br substituent from the pyrazino group, which parallels the formation of compound **9** by Ni insertion in DMF. The hemiporphycenes have a smaller HOMO−LUMO gap, and they are always easier to reduce than the corresponding porphyrin complexes. These features make these compounds of interest for applications for example as sensing layers in chemical sensors, and this study is currently ongoing in our laboratories.

ASSOCIATED CONTENT

Supporting Information

FAB-MS, ^{1}H and ^{13}C NMR spectra, COSY, HSQC, HMBC spectra of **4**. FAB-MS and ^{1}H NMR spectra of compounds. This material is available free of charge via the Internet at http://pubs.acs.org

AUTHOR INFORMATION

Corresponding Authors

*(R.P.) E-mail: roberto.paolesse@uniroma2.it.
*(K.M.K.) E-mail: kkadish@uh.edu.

Notes

The authors declare no competing financial interest.

ACKNOWLEDGMENTS

MIUR is gratefully acknowledged for financial support (Project PRIN 2009Z9ASCA). Support of the Robert A. Welch Foundation (KMK, Grant E-680) is gratefully acknowledged.

REFERENCES

(1) (a) *The Porphyrin Handbook*; Kadish, K. M., Smith, K. M., Guilard, R., Eds.; Academic Press: San Diego, CA, 2000; Vol. *2*, pp 121−214. (b) Paolesse, R. *Synlett* **2008**, 2215.
(2) (a) Aviv-Harel, I.; Gross, Z. *Chem.—Eur. J.* **2009**, *15*, 8382. (b) Flamigni, L.; Gryko, D. T. *Chem. Soc. Rev.* **2009**, *38*, 1635. (c) Tortora, L.; Pomarico, G.; Nardis, S.; Martinelli, E.; Catini, A.; D'Amico, A.; Di Natale, C.; Paolesse, R. *Sens. Actuators B* **2013**, *187*, 72.
(3) (a) Paolesse, R.; Jaquinod, L.; Nurco, D. J.; Mini, S.; Sagone, F.; Boschi, T.; Smith, K. M. *Chem. Commun.* **1999**, 1307. (b) Gross, Z.; Galili, N.; Saltsman, I. *Angew. Chem., Int. Ed.* **1999**, *38*, 1427.
(4) (a) Paolesse, R.; Nardis, S.; Sagone, F.; Khoury, R. G. *J. Org. Chem.* **2001**, *66*, 550. (b) Gryko, D. T.; Koszarna, B. *Org. Biomol. Chem.* **2003**, *1*, 350. (c) Paolesse, R.; Marini, A.; Nardis, S.; Froiio, A.; Mandoj, F.; Nurco, D. J.; Prodi, L.; Montalti, M.; Smith, K. M. *J. Porphyrins Phthalocyanines* **2003**, *7*, 25. (d) Koszarna, B.; Gryko, D. T. *J. Org. Chem.* **2006**, *71*, 3707.
(5) Barata, J. F. B.; Santos, C. I. M.; Neves, M. G. P. M. S.; Amparo, M. A. F.; Cavaleiro, J. A. S. in *Synthesis and Modification of Porphyrinoids − Topics in Heterocyclic Chemistry*; Paolesse, R., Ed.; Springer: New York, 2014; Vol. *33*, pp 79−141.
(6) (a) Scrivanti, A.; Beghetto, V.; Matteoli, U.; Antonaroli, S.; Marini, A.; Mandoj, F.; Paolesse, R.; Crociani, B. *Tetrahedron Lett.* **2004**, *45*, 5861. (b) Gao, D.; Canard, G.; Giorgi, M.; Balaban, T. S. *Eur. J. Inorg. Chem.* **2012**, 5915.
(7) (a) Aviv-Harel, I.; Gross, Z. *Chem. Commun.* **2007**, 1987. (b) Flamigni, L.; Gryko, D. T. *Chem. Soc. Rev.* **2009**, *38*, 1635. (c) Paolesse, R.; Monti, D.; Nardis, S.; Di Natale, C. In *Handbook of Porphyrin Science*; Kadish, K. M.; Smith, K. M.; Guilard, R., Eds.; World Scientific Publishing: Singapore, 2011; Vol. *12*, pp 121−214.
(8) Barata, J. F. B.; Silva, A. M. G.; Faustino, M. A. F.; Neves, M. G. M. S.; Tomè, A. C.; Silva, A. M. S.; Cavaleiro, J. A. S. *Synlett* **2004**, *7*, 1291.
(9) Zhao, S. Z.; Neves, M. G. P. M.; Tomé, A. C.; Silva, A. M. S.; Cavaleiro, J. A. S.; Domingues, M. R. M.; Correia, A. J. F. *Tetrahedron Lett.* **2005**, *46*, 2189.
(10) Paolesse, R.; Nardis, S.; Stefanelli, M.; Fronczek, F. R.; Vicente, M. G. H. *Angew. Chem., Int. Ed.* **2005**, *44*, 3047.
(11) (a) Mandoj, F.; Stefanelli, M.; Nardis, S.; Mastroianni, M.; Fronczek, F. R.; Smith, K. M.; Paolesse, R. *Chem. Commun.* **2009**, 1580. (b) Mandoj, F.; Nardis, S.; Pomarico, G.; Stefanelli, M.; Schiaffino, L.; Ercolani, G.; Prodi, L.; Genovese, D.; Zaccheroni, N.; Fronczek, F. R.; Smith, K. M.; Xiao, X.; Shen, J.; Kadish, K. M.; Paolesse, R. *Inorg. Chem.* **2009**, *48*, 10346.
(12) Singh, P.; Dutta, G.; Goldberg, I.; Mahammed, A.; Gross, Z. *Inorg. Chem.* **2013**, *52*, 9349.
(13) Stefanelli, M.; Mastroianni, M.; Nardis, S.; Licoccia, S.; Fronczek, F. R.; Smith, K. M.; Zhu, W.; Ou, Z.; Kadish, K. M.; Paolesse, R. *Inorg. Chem.* **2007**, *46*, 10791.
(14) Gros, C. P.; Barbe, J.-M.; Espinosa, E.; Guilard, R. *Angew. Chem., Int. Ed.* **2006**, *45*, 5642.
(15) Palmer, J. H.; Brock-Nannestad, T.; Mahammed, A.; Durrell, A. C.; VanderVelde, D.; Virgil, S.; Gross, Z.; Gray, H. B. *Angew. Chem., Int. Ed.* **2011**, *50*, 9433.
(16) Senge, M. O.; Sergeeva, N. N. *Angew. Chem., Int. Ed.* **2006**, *45*, 7492.
(17) Nardis, S.; Stefanelli, M.; Mohite, P.; Pomarico, G.; Tortora, L.; Manowong, M.; Chen, P.; Kadish, K. M.; Fronczek, F. R.; McCandless, G. T.; Smith, K. M.; Paolesse, R. *Inorg. Chem.* **2012**, *51*, 3910.

(18) Stefanelli, M.; Pomarico, G.; Tortora, L.; Nardis, S.; Fronczek, F. R.; McCandless, G. T.; Smith, K. M.; Manowong, M.; Fang, Y.; Chen, P.; Kadish, K. M.; Rosa, A.; Ricciardi, G.; Paolesse, R. *Inorg. Chem.* **2012**, *51*, 6928.
(19) Cai, X.; Donzello, M. P.; Viola, E.; Rozzoli, C.; Ercolani, C.; Kadish, K. M. *Inorg. Chem.* **2009**, *48*, 7066.
(20) Insian, C.; Saillard, J.-Y.; Guilard, R.; Tabard, A.; Mest, Y. L. *New. J. Chem.* **1998**, 823.
(21) Kadish, K. M.; Ou, Z.; Zhan, R.; Khoury, T.; Crossley, M. J. *J. Porphyrins Phthalocyanines* **2010**, *14*, 866.